Multilayer Microstrip Structure Analysis with Matched Load Simulation

Edwin K. L. Yeung, John C. Beal, *Member, IEEE,* and Yahia M. M. Antar, *Senior Member, IEEE*

Abstract— **This paper presents a generalized approach to the full-wave analysis of multilayer microstrip structures. One of the structures studied is a new kind of microstrip bandpass filter realized in a double-layer dielectric substrate configuration. This filter demonstrates the use of the third (vertical) dimension in the design of microstrip devices. The approach involves the mixed potential integral equation technique, the Method of Moments, and an S-parameter extraction technique based on a simple form of Matched Load Simulation. Simulated and measured results for various microstrip structures are presented and show good agreement. The approach is demonstrated in detail for 2-port structures, with an outline of how it can readily be extended to the n-port case.**

I. Introduction

MULTILAYER microstrip circuits offer the advantage of greater compactness and lend themselves to incorporation in monolithic integrated circuits. This paper introduces a new kind of microstrip filter consisting of a microstrip line with a gap and a parasitic resonator line mounted on a second layer above the gap. Extension to other forms is also considered. Analysis is facilitated by the use of a simulated matched load on the output port thereby enabling the direct calculation of the S-parameters for the device. For the full-wave analysis of microstrip structures, the most popular approach involves an integral equation formulation and the application of Method of Moments (MOM) [1]. Over the past decade, with the acceleration of computing capability, numerous researchers have reported reliable simulation results for characterizing planar microstrip discontinuities, e.g. [2]–[9]. In addition, the numerical analysis of physical configurations consisting of multiple layers of substrate and metallization has become possible, e.g. [10]–[12]. Although the use of the third (vertical) dimension in the design of microstrip components remains a fairly new subject, some previous examples include the overlay directional coupler [13], the semi-reentrant coupler [14], slot couplers [12], [15], and novel proximity couplers [6].

Manuscript received August 2, 1993; revised February 17, 1994. The authors wish to acknowledge Sharon Aspden of the Rogers Corporation for their supply of microwave materials used in this work, which was partially supported by the Natural Sciences and Engineering Research Council and the Department of National Defence, Canada.

E. K. L. Yeung is with the Department of Electrical and Computer Engineering, Royal Military College of Canada, Kingston, ON, K7K 5L0, Canada.

J. C. Beal is with the Department of Electrical Engineering, Queen's University, Kingston, ON, K7L 3N6, Canada.

Y. M. M. Antar is with the Department of Electrical and Computer Engineering, Royal Military College of Canada, Kingston, ON, K7K 5L0, Canada, and holds an adjunct position in the Department of Electrical Engineering, Queen's University, Kingston, ON, K7L 3N6, Canada.

IEEE Log Number 9406799.

In this paper, an approach to the full-wave analysis of open double layer two-port microstrip discontinuities is presented. This approach is suitable for treating double-layer planar discontinuities as shown in Fig. 1. The discontinuities presented include an embedded microstrip gap (Fig. 2(a)), a microstrip gap with offset overlay resonator (Fig. 2(b)) and a derived novel double layer microstrip bandpass filter (Fig. 2(c)). The analysis is based on the Mixed Potential Integral Equation (MPIE) [16] and MOM is applied in the spatial domain. Thus radiation, surface waves and mutual coupling are all included. Dielectric loss is also accounted for as it is included in the formulation of the Green's functions. A Matched Load Simulation (MLS) technique [17] is then introduced for the extraction of S-parameters from the current distribution. While this technique can be seen to be broadly similar to that in other work, such as [3] to [10], in that it represents travelling waves on the output microstrip lines, it is here presented explicitly in the spatial domain with a process of enforcement of relative current values on a small number of elements along the output line. As the whole treatment of the network is here also in the spatial domain, this provides a very simple way to simulate a matched load on the output port.

An independent work [18] has also recently proposed a method of matched load simulation by the inclusion of loaded scatterers on the output line of a two-port network. However, the MLS technique now introduced, with its direct enforcement of current amplitude and phases, appears to be significantly more efficient and simpler to implement.

Since all of the structures analyzed here have small transverse dimensions compared to the wavelength, the transverse components of current are considered second order effects, as in [3], and are ignored. Conductor loss and thickness are not accounted for as they have negligible effects in the frequency range of interest.

II. Analysis

A. Formulation

The MPIE has been applied by many authors to treat microstrip antennas and discontinuities, e.g. [19]–[22]. The present formulation is adapted from that in [16]. In Fig. 1, the boundary condition of the tangential electric field on the conductive surfaces on both interfaces can be written as:

$$\boldsymbol{E}_t^e(\boldsymbol{r}) = -\boldsymbol{E}_t^s(\boldsymbol{r}) = (j\omega \boldsymbol{A}(\boldsymbol{r}) + \nabla V(\boldsymbol{r}))_t \qquad (1)$$

where the superscripts e, s, and the subscript t represent excited, scattered and tangential components, respectively. The

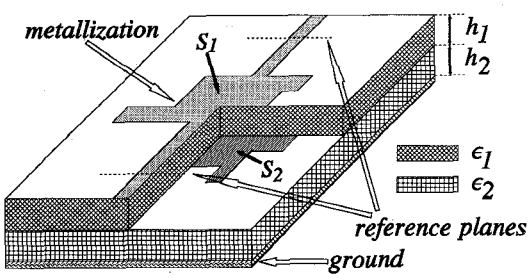

Fig. 1. An arbitrary two-port double-layer microstrip discontinuity with defined reference planes.

potentials $\boldsymbol{A}$ and V can be written as:

$$\boldsymbol{A}(\boldsymbol{r}) = \int_{S_1+S_2} \boldsymbol{G_A}(\boldsymbol{r}|\boldsymbol{r}') \cdot \boldsymbol{J}_s(\boldsymbol{r}')\, d\boldsymbol{r}' \tag{2}$$

$$V(\boldsymbol{r}) = \int_{S_1+S_2} G_V(\boldsymbol{r}|\boldsymbol{r}')\rho_s(\boldsymbol{r}')\, d\boldsymbol{r}' \tag{3}$$

$\boldsymbol{G_A}$ and G_V are Green's functions for the magnetic vector potential and the electric scalar potential, respectively, for a horizontal electric dipole and expressions for them, in the form of Sommerfeld integrals, are listed explicitly in [16]. With numerical integration in the complex plane, these Green's functions are obtained as functions of radial distance. They are then tabulated for a chosen set of discrete positions and interpolated as needed by use of a cubic spline, as demonstrated in [23].

B. Method of Moments

As the boundary condition is enforced on the conductive surfaces, a two dimensional MOM procedure is applied and the conductive surfaces are discretized into rectangular cells. Overlapping roof-top basis functions [24] and two-dimensional pulse functions are used for the expansion of the surface current density, $\boldsymbol{J}_s$, and the surface charge density, ρ_s, respectively. For the testing procedure, one-dimensional pulse functions (or razor functions) are used. These choices of basis functions and testing functions are based on their compatibility with the MPIE [19] and lead to the efficient evaluation of the terms in the moment matrix. The MPIE is thus transformed into a matrix equation:

$$\sum_{j=1}^{N} Z_{i,j} \cdot I_j = V_i, \qquad i = 1, 2, \cdots, N \tag{4}$$

where the $Z_{i,j}$ represent interactions between the cells on the metallized surfaces, I_j are the unknown current expansion coefficients, and V_i are the excitations.

C. Treatment of Input Port

For multi-port microstrip discontinuities, the input and output reference planes have to be specified. As shown in Fig. 1, the reference planes are defined for a two port, arbitrarily shaped, double-layer discontinuity. For excitation, a delta gap generator is placed sufficiently far away from the input reference plane to allow for an undisturbed current standing wave (SW) to appear along the input line, as in [3]. S-parameters can then be obtained directly from this current SW when all the output lines are matched.

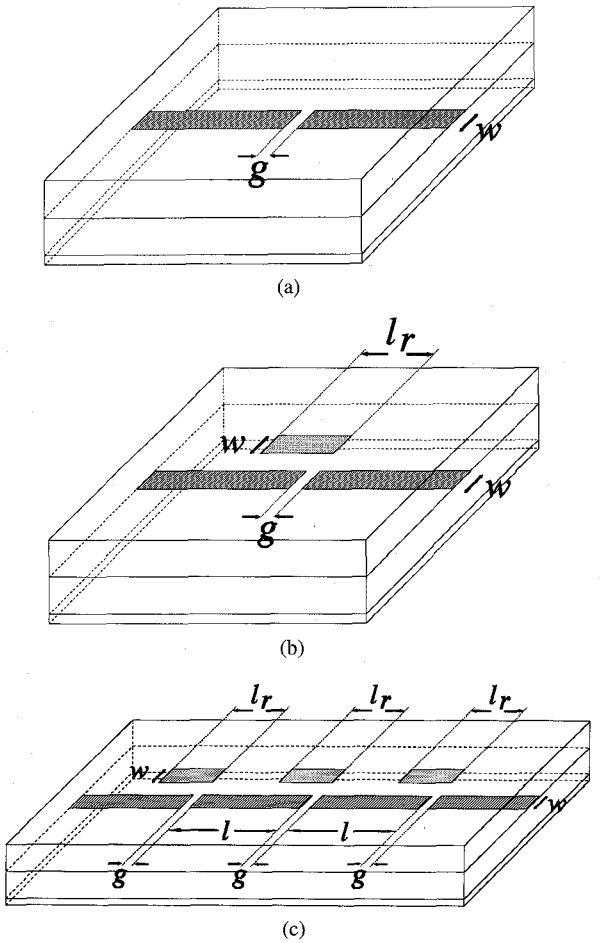

Fig. 2. Two port discontinuities studied : (a) an embedded microstrip gap, (b) an embedded microstrip gap with an overlay half-wave microstrip resonator (MGOHR), and (c) a novel double-layer microstrip bandpass filter (DLMBPF); light shading area: metallization at air-dielectric interface, heavy shading area: metallization at dielectric-dielectric interface.

D. Treatment of Output Ports

We apply matched load simulation (MLS) to the output ports. Specifically, we simulate matched load terminations at the output ports by enforcing in the spatial domain a unidirectional current travelling wave propagating along each of the output lines in the direction away from the discontinuities. The simulation is based on a simple manipulation of the matrix equation (4). There are two figways of manipulating the equation to achieve the same matched load effects.

The first way, introduced in [17] for a two-port discontinuity, involves the specification of some current coefficients at the end of the output line. If the total number of unknown coefficients and the number of coefficients to be specified are N and k, respectively, the specification can be generalized as:

$$I_{N-(k-m)} = e^{-j(m-1)\beta_g l}, \qquad m = 1, 2, \cdots, k \tag{5}$$

where β_g is the pre-computed propagation constant for the output line and l is the distance between the locations of the centers of successive roof-top basis functions. The number of unknown coefficients is now reduced to $N - k$ and therefore only $(N - k + 1)$ equations are needed. The extra equation is for solving for the delta-gap voltage as this is no longer arbitrary but is related to the specified coefficients. To reflect

this enforced current condition in the matrix equation (4), the specified coefficients and their corresponding entries in the $Z_{i,j}$ matrix may be considered as effective sources and can then be re-arranged to form a new excitation vector to replace $[V_i]$. The matrix equation now becomes:

$$\begin{bmatrix} Z_{1,1} & \cdots & Z_{1,N-k} & -1 \\ \vdots & \ddots & \vdots & \vdots \\ Z_{N-k,1} & \cdots & Z_{N-k,N-k} & 0 \\ Z_{N-k+1,1} & \cdots & Z_{N-k+1,N-k} & \vdots \end{bmatrix} \begin{bmatrix} I_1 \\ \vdots \\ I_{N-k} \\ V_1 \end{bmatrix} = \begin{bmatrix} E_1 \\ \vdots \\ \vdots \\ E_{N-k+1} \end{bmatrix} \tag{6}$$

where

$$E_i = -\sum_{j=N-k+1}^{N} Z_{i,j} I_j$$

The E_i's are these newly formed effective sources. Obviously, for multi-port discontinuities, the relationships among the currents on each matched output line are generally unknown. Thus, in the multi-port case, the coefficients on each output line would have to be specified accordingly; i.e., they would initially be completely known on only one output line, with the relative amplitudes of the currents on the other output lines to be included among the unknowns in the matrix equation.

The second way of implementing MLS is even simpler and better suited for multi-port simulation. No re-arrangements of matrix terms are required. The mutual relationship of the current coefficients along the various output lines is enforced by introducing new linear equations into the matrix equation such as:

$$I_m - I_{m+1} e^{-j\beta_g l} = 0 \tag{7}$$

This equation enforces a uniform magnitude and a uniform progressive phase lag constraint on the coefficients I_m and I_{m+1} on any particular output line. With the previous assumptions of N and k, a typical mth row in $Z_{i,j}$ for $m \geq N-k+1$ now becomes:

$$[0 \cdots 0 \quad 1 \quad -e^{j\beta_g l} \quad 0 \cdots 0] \tag{8}$$

The advantage of this implementation of MLS over the previous one lies in the fact that the magnitudes and phases of the currents on all the matched output lines are now obtained as the solution of the matrix equation. The delta gap voltage can thus be arbitrarily chosen, as in the case of a one-port network.

Investigation has shown that the above two procedures for the implementation of MLS do satisfactorily simulate matched loads at the output ports. Consequently, the solution obtained to the new matrix equation does approximate, to a high degree, the current distribution on the whole structure when all ports are truly matched, thus enabling the S-parameters to be directly found.

It is important to stress that constant-amplitude, constant phase-lag current conditions should only be enforced for coefficients associated with current cells that are physically located far from the discontinuity at the junction between the output line and the device. This ensures that all effects due to the discontinuity will have become negligible and that the enforcement of a simple outgoing quasi-TEM mode is then justified. Numerical trials have shown that the enforcement region should be at least a quarter-wavelength from the junction discontinuity.

E. Derivation of S-parameters

Once the current distribution of a matched multi-port structure has been obtained, the extraction of S-parameters involves only basic transmission line theory. The magnitudes of the S-parameters for a multi-port network are given by:

$$|S_{11}| = \frac{I_{\max} - I_{\min}}{I_{\max} + I_{\min}} \qquad |S_{i1}| = \frac{2|I_i|}{I_{\max} + I_{\min}}, \qquad i \neq 1 \tag{9}$$

where $I_{\max}$ and $I_{\min}$ are the current maximum and minimum, respectively, of the SW pattern on the input line and $|I_i|$ is the current magnitude at the ith output reference plane. The phase of S_{11} is obtained from the well known procedure [3] of locating the nearest current minimum of the SW pattern and finding its distance from the input reference plane. The phase of S_{i1} for i other than 1 is then given by:

$$\angle S_{i1} = \angle I_i - \angle \frac{I_{\text{in}}}{1 - S_{11}}, \qquad i \neq 1 \tag{10}$$

where I_{in} is the complex current at the input reference plane.

$I_{\max}$ and $I_{\min}$ are obtained through the use of cubic spline interpolation [25] of a discretized SW pattern. The error introduced in the interpolation is generally much higher at the minima than at the maxima. However, with the use of MLS, in which power is simulated as being absorbed at the outputs, an accurate estimation of the current minimum can be achieved with a moderate cell density (100 cells per λ_g). This constitutes a further advantage in the use of MLS in that the minima are much easier to estimate than when o/c terminations [26] are used on the output lines, particularly for low-loss networks for which the input SWR will be close to infinite for an o/c at the output.

To obtain S_{ij} (including $j = i$) for i other than 1, the delta gap excitation must be placed at line i while MLS is applied to all other lines. For N-port discontinuities, the maximum possible number of distinct S-parameters is N^2. However, in most practical cases, symmetry and reciprocity considerations greatly reduce the number of distinct S-parameters to be derived.

III. VERIFICATION

A. Uniform Microstrip Line

MLS is first applied to a uniform microstrip line on its own so that the effects of the number of cells enforced, and of the cell density, on the simulated behavior can be studied. The microstrip line (Fig. 3) is treated as a two-port structure with the excitation, V, at one end of the strip and MLS applied

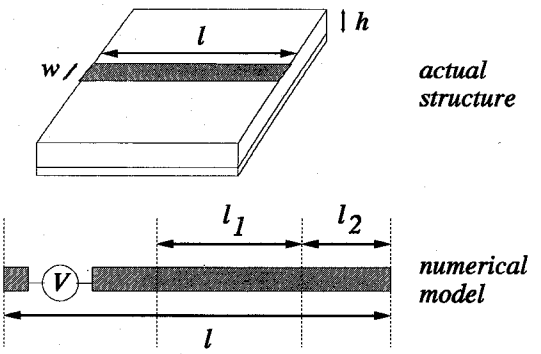

Fig. 3. A uniform microstrip line and its numerical model.

along l_2 at the other end. We are interested in studying the resulting current coefficients on l_1 as N_e, the number of coefficients enforced on l_2, is varied. The simulated current magnitudes for various N_e are shown in Fig. 4(a) [17]. For the case of $N_e = 8$, the results have achieved an accuracy within 1.0% of the theoretical value of 1.0 A. The residual periodic behavior is believed to be caused by the finite value of N_e. Similar accuracy is obtained for the phase relationship as depicted in Fig. 4(b) (theoretical phase-lag ≈3.3°). This value of N_e, for example, corresponds for the dimensions tested to approximately 110 coefficients per wavelength at the specified frequency of 2 GHz. At higher frequencies it is anticipated that the same number per wavelength would suffice for effective matched load simulation. It should, however, be noted that the MPIE formulation itself would have to be extended (e.g., to include transverse currents) if the frequency were increased sufficiently; whether this simple form of MLS could then still be used would require further investigation.

For a varying cell density, similar results show that higher cell densities produce simulated currents with magnitudes and phases closer to the theoretical values (for an approximately constant total enforced length, l_2) [26].

B. Microstrip Gap

As a further test of the usefulness of the MLS approach, the simulated and measured magnitudes of the S-parameters for a microstrip gap embedded in RT-duroid (Fig. 2(a)) are shown in Fig. 5. The line widths are chosen to achieve a 50 Ω guiding structure to simplify the measurement. Although the magnitude of S_{21} is inherently small and therefore susceptible to device tolerances and measurement errors, the agreement between the simulated and measured results does indeed confirm the usefulness of this simple form of MLS.

IV. Application to Novel Filter Structures

A. Microstrip Gap with Overlay Half-Wave Resonator (MGOHR)

The addition of a parasitic microstrip half-wavelength resonator above the gap introduces novel filtering possibilities and suggests an important way to make use of the third dimension in multi-layer microstrip structures. For the simplest case with the resonator symmetrically over the gap with no offset (i.e. $s = 0$ in Fig. 6), the results are shown in Fig. 7(a) for the

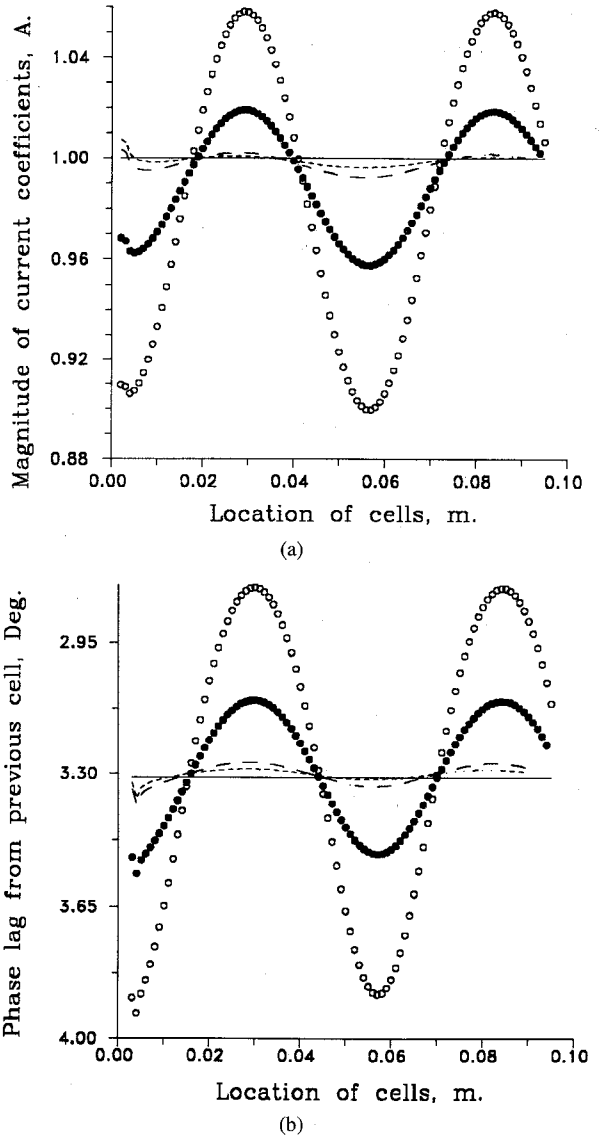

Fig. 4. Currents on a simulated matched uniform microstrip line : (a) Magnitudes, (b) Phase-lag; o: $N_e = 4$, •: $N_e = 5$, — — — ; $N_e = 8$, - - - - : $N_e = 10$, _____: Theory; N_e = number of enforced cells ($w = h =$ 1.0 mm, $\epsilon_r = 2.3$, frequency = 2.0 GHz).

magnitudes of the S-parameters, and in Fig. 7(b) for their phases. The magnitude results (Fig. 7(a)) show a very good agreement (measured $|S_{11}|_{\min} \approx -26$ dB) at the frequency (4.0 GHz) at which the overlay resonator is a half-wavelength long. The coupling, S_{21}, is much stronger for the entire frequency range (2.0 to 6.0 GHz) than when without the overlay resonator (Fig. 5) and peaks at around 4.0 GHz. The simulated phase results (Fig. 7(b)) show a linear behavior for S_{21} which is desirable if signal distortion is to be minimized. This frequency selective behavior promises the possibility of a new class of 3-dimensional microstrip filters. We note that the designable parameters for this structure include the gap width g, the resonator length l_r, and the resonator offset s, which is measured from the center of the resonator to the center of the microstrip line (Fig. 6). This offset is found to be useful in controlling the steepness of the $|S_{21}|$ response, as discussed later.

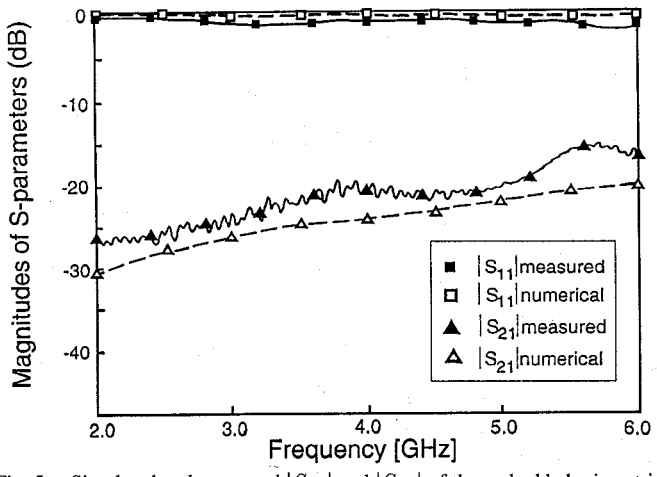

Fig. 5. Simulated and measured $|S_{11}|$ and $|S_{21}|$ of the embedded microstrip gap in Fig. 2(a) ($\epsilon_{r1} = \epsilon_{r2} = 2.33, h_1 = h_2 = 0.8382$ mm, $w = 2.3$ mm, $g = 1.0$ mm).

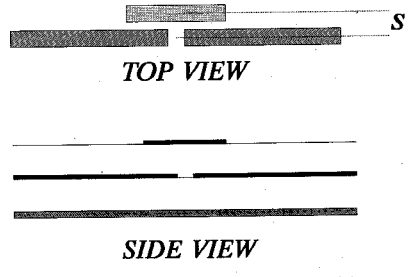

Fig. 6. Top view and side view of a microstrip gap with an overlay resonator showing the lateral offset, s (light shading: metallization at air-dielectric interface, heavy shading: metallization at dielectric-dielectric interface).

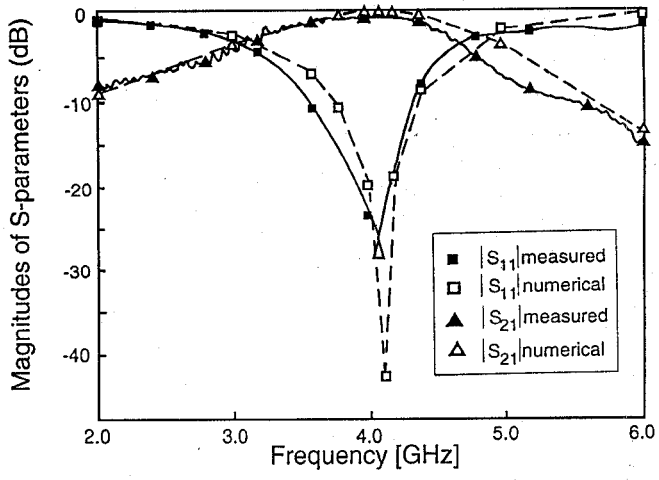

(a)

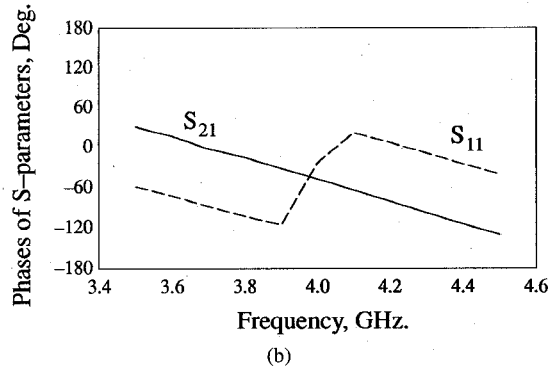

(b)

Fig. 7. S_{11} and S_{21} of a MGOHR with a zero-offset ($s = 0$) overlay half-wave resonator (Fig. 2(b)): (a) simulated and measured magnitudes, (b) simulated phases ($\epsilon_{r1} = \epsilon_{r2} = 2.33, h_1 = h_2 = 0.8382$ mm, $w = 2.3$ mm, $g = 1.0$ mm, $l_r = 27.3$ mm).

The gap width g, is found to have very little effect on the overall response of the structure [26], except for a slight shift of the center frequency. The effect of a varying gap width on the center frequency is tabulated in Table I. A slight down shift of the center frequency is observed as the gap width is increased and is correctly predicted by the simulations for various values of g and l_r. From a design perspective, a shift in the center frequency can also be produced by a change in l_r. This is an improved way of designing the center frequency as the change is more predictable, as shown in Table I. l_r is a half-wavelength at the design frequency, where the wavelength refers to the one for a uniform microstrip line of width w and height of $(h_1 + h_2)$. As such, the end effects for the resonator are not accounted for in the design and thus the actual center frequency can be expected to be slightly smaller than the designed one.

A very interesting improvement in the steepness of the skirt selectivity for $|S_{21}|$ is obtainable by laterally offsetting the overlay resonator (i.e., $s > 0$ in Fig. 6) to a small extent. The effect is similar to that of decreasing the coupling to a tuned circuit. The simulated results for a microstrip gap with an offset overlay half-wave resonator are depicted in Fig. 8(a), together with the experimental measurement for the $s = 0.5$ w case. They show a decrease in the off-center value of $|S_{21}|$ at 4.5 GHz from approximately -1.5 dB to -11 dB as s is increased from 0 w to 0.75 w (1.73 mm). This decrease is associated with a tolerably small reduction in the $|S_{21}|$ peak

TABLE I
COMPARISON OF MEASURED AND SIMULATED CENTER FREQUENCIES OF A MGOHR (FIG. 2(b)) WITH VARIOUS g AND l_r COMBINATIONS. (PHYSICAL PARAMETERS AS IN FIG . 7)

g [mm]	l_r [mm]	designed centre frequency [GHz]	measured centre frequency [GHz, ± 5 MHz	simulated centre frequency [Ghz] ± 50 MHz	% difference between measured & simulated
1.0	27.3	4.0	4.070	4.10	0.74
5.0	27.3	4.0	3.770	3.90	3.4
5.0	28.74	3.8	3.640	3.75	3.0
10.0	28.74	3.8	3.510	3.55	1.1
5.0	26.0	4.2	3.895	4.05	4.0
10.0	26.0	4.2	3.830	3.95	3.1

at approximately 4 GHz. As indicated in the $|S_{11}|$ results in Fig. 8(b), including the experimental measurement for the $s = 0.5$ case, the center frequency is also slightly down shifted as s increases. This behavior may be caused by an increase in the end capacitances for an offset resonator compared to a zero-offset one, since the embedded microstrip may have a bigger field-confining effect on a zero-offset resonator. An offset s of 0.75 w is a good choice for filter design since it retains the good match while providing a steep roll-off on either side of the center frequency.

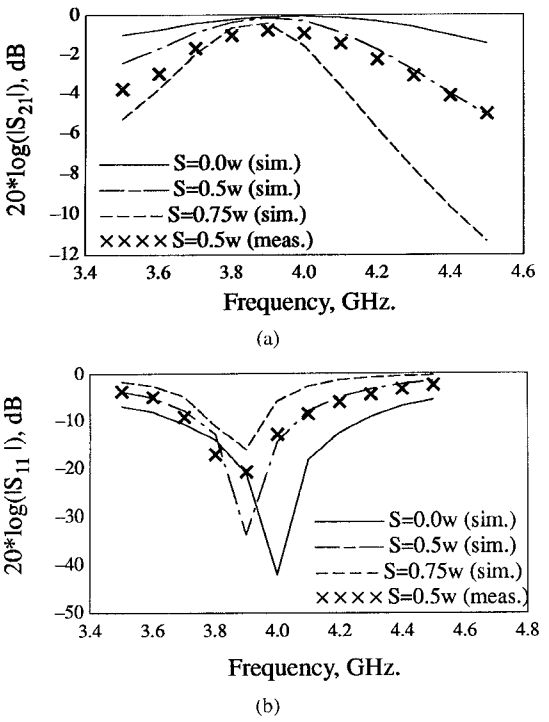

Fig. 8. Simulated and measured magnitudes of S-parameters of a MGOHR with an offset overlay resonator (Fig. 2(b)), s = 0.0, 0.5 w and 0.75 w: (a) $|S_{21}|$, (b) $|S_{11}|$ (physical parameters as in Fig. 7).

A similar analysis was performed for a microstrip gap with an underlay half-wavelength microstrip resonator [26]. The results obtained (not shown here) were comparable to those in Figs. 7 and 8, and Table I.

The presence of the parasitic resonator might be expected to produce radiation in the upper half space. In fact this is not the case to any significant extent, as is shown, both numerically and experimentally, by the closeness of the $|S_{21}|$ value to 0 dB at the center frequency (Figs. 7(a) and 8(a)). The effective absence of radiation must be attributable to the close coupling to the continuing microstrip line.

B. Double-Layer Microstrip Bandpass Filter (DLMBPF)

This configuration is based on cascading a number of identical MGOHR sections. An example of it is depicted in Fig. 2(c) and consists of 3 sections. The cascading produces a further improvement in the steepness of the $|S_{21}|$ response over that of a single MGOHR, provided that a suitable intersection spacing $(l + g)$ is used. The design of DLMBPF involves the characterization of a MGOHR using MLS. Then the ABCD matrix is obtained from the S-matrix of a MGOHR for cascading purposes. Thus, the coupling between successive resonators, beyond that along the microstrip lines, is ignored, which is valid if they are sufficiently far apart. Therefore the approach for the analysis of DLMBPF is a hybrid one that involves full-wave analysis (for a single MGOHR) and network theory (for cascading network parameters).

The optimum section spacing for the best filtering characteristics of the cascaded structure, is found by numerical trials to be an odd multiple of a quarter wavelength at the center frequency. The use of $3\lambda_g/4$ for the section spacing

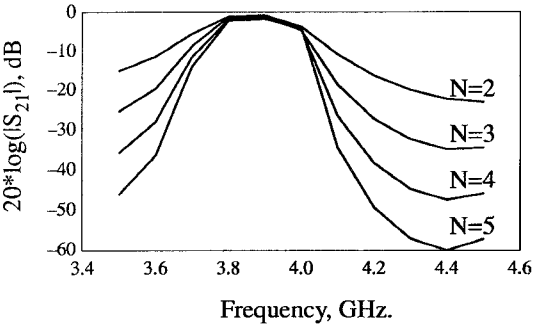

Fig. 9. Simulated $|S_{21}|$ of a DLMBPF (Fig. 2(c)) for a varying number of cascaded sections N (N = 2 to 5, s = 0.75 w for all sections, l = 38.6 mm, other physical parameters as in Fig. 7).

is the practical minimum as the resonators would then be approximately $\lambda_g/4$ apart. With this section spacing of $3\lambda_g/4$, the overall S-parameters for cascading 2 to 5 sections are depicted in Fig. 9 showing the dramatic steepening of the skirts of $|S_{21}|$. However, the overall $|S_{21}|$ peak drops to approximately -2.5 dB in the 5-section case. Thus a trade-off of transmission peak and skirt steepness is again observed. In general, the amount of offset s and the number of sections can thus be optimized to create a desired filter function. Experimental verification of the simulated responses is in progress. It is worth noting that the overall length of a 3-section filter of this proposed new kind is only about 5 cm on duroid (ϵ_r = 2.8), for a center frequency of 10 GHz.

Other possible forms are worthy of investigation, including increasing the number of layers with resonant overlays, or underlays, or adding offset overlay elements on either side of the gap. There thus arises the potential for truly 3 dimensional microstrip filters.

V. Conclusion

In this paper, we have presented an approach to the full-wave analysis of multi-layer, two-port microstrip discontinuities with an outline of the possible extension to n-port networks. The approach involves the mixed potential integral equation, the Method of Moments, and a very simple Matched Load Simulation technique. The technique allows straightforward extraction of the S-parameters for the discontinuities from the solution of the integral equation. For design purposes, the overall characteristics of a combination of various discontinuities in series can be obtained through the cascading of the parameters for the individual structures. This combination of full-wave analysis and a network approach for the analysis of complicated structures is efficient while still accounting for the dominant electromagnetic effects.

Test simulation results for the isolated microstrip line itself are convincing and those for the embedded microstrip gap compare well with measurements. A novel double-layer microstrip filter structure has been introduced, with good agreement between the simulated and measured results. This builds on the selective coupling across a microstrip gap produced by an offset overlay half-wave microstrip resonator. This structure opens up the possibility of a new class of 3-dimensional microstrip filters.

ACKNOWLEDGMENT

The authors wish to thank Capt. Serge Couture, and Dr. A. Ittipiboon and M. Cuhaci of the Communications Research Centre, Ottawa, Canada for their many valuable suggestions and discussions.

REFERENCES

[1] R. F. Harrington, *Field Computation by Moment Methods*. New York: MacMillan, 1968.
[2] J. S. Hornsby, "Full-wave analysis of microstrip resonator and open-circuit end effects," *IEE Proc. Microwaves, Opt. & Antennas*, vol. 129, Pt. H, pp. 338–341, Dec. 1982.
[3] P. B. Katehi and N. G. Alexopoulos, "Frequency-dependent characteristics of microstrip discontinuities in millimeter-wave integrated circuits," *IEEE Trans. Microwave Theory Tech.*, vol. MTT-33, pp. 1029–1035, Oct. 1985.
[4] R. W. Jackson and D. M. Pozar, "Full-wave analysis of microstrip open-end and gap discontinuities," *IEEE Trans. Microwave Theory Tech.*, vol. MTT-33, pp. 1036–1042, Oct. 1985.
[5] R. H. Jansen, "The spectral-domain approach for microwave integrated circuits," *IEEE Trans. Microwave Theory Tech.*, vol. MTT-33, pp. 1043–1056, Oct. 1985.
[6] H.-Y. Yang and N. G. Alexopoulos, "Basic blocks for high-frequency interconnects: Theory and experiment," *IEEE Trans. Microwave Theory Tech.*, vol. MTT-36, pp. 1258–1264, Aug. 1988.
[7] R. W. Jackson, "Full-wave, finite element analysis of irregular microstrip discontinuities," *IEEE Trans. Microwave Theory Tech.*, vol. MTT-37, pp. 81–89, Jan. 1989.
[8] S.-C. Wu, H.-Y. Yang, N. G. Alexopoulos, and I. Wolff, "A rigorous dispersive characterization of microstrip cross and T junctions," *IEEE Trans. Microwave Theory Tech.*, vol. MTT-38, pp. 1837–1844, Dec. 1990.
[9] T.-S. Horng, W. E. McKinzie, and N. G. Alexopoulos, "Full-wave spectral-domain analysis of compensation of microstrip discontinuities using triangular subdomain functions," *IEEE Trans. Microwave Theory Tech.*, vol. MTT-40, pp. 2137–2147, Dec. 1992.
[10] H.-Y. Yang, N. G. Alexopoulos, and D. R. Jackson, "Microstrip open-end and gap discontinuities in a substrate-superstrate structure," *IEEE Trans. Microwave Theory Tech.*, vol. MTT-37, pp. 1542–1546, Oct. 1989.
[11] W. P. Harokopus, Jr. and P. B. Katehi, "Charaterization of microstrip discontinuities on multilayer dielectric substrates including radiation losses," *IEEE Trans. Microwave Theory Tech.*, vol. MTT-37, pp. 2058–2066, Dec. 1989.
[12] W. Schwab and W. Menzel, "On the design of planar microwave components using multilayer structures," *IEEE Trans. Microwave Theory Tech.*, vol. MTT-40, pp. 67–72, Jan. 1992.
[13] H. R. Malone, "Microstrip overlay coupler suits broadband use," *Microwaves & RF Mag.*, pp. 84–86, July 1985.
[14] M. Nakajima and E. Yamashita, "A quasi-TEM design method for 3-dB hybrid couplers using a semi-reentrant coupling section," *IEEE Trans. Microwave Theory Tech.*, vol. MTT-38, pp. 1731–1733, Nov. 1990.
[15] M .W. Katsube, Y. M. M. Antar, A. Ittipiboon, and M. Cuhaci, "A novel aperture coupled microstrip 'Magic-T'," *IEEE Microwave and Guided Wave Lett.*, vol. 2, pp. 245–246, June 1992.
[16] L. Barlatey, J. R. Mosig, and T. Sphicopoulos, "Analysis of stacked microstrip patches with a mixed potential integral equation," *IEEE Trans. Antenn. Propagat.*, vol. AP-38, pp. 608–615, May 1990.
[17] E. K. L. Yeung, J. C. Beal, and Y. M. M. Antar, "Matched load simulation for multiport microstrip structures," *Electron. Lett.*, vol. 29, no. 10, pp. 867–868, May 13, 1993.
[18] H. Ghali, M. Drissi, J. Citerne, and V. Fouad Hanna, "Numerical simulation of a virtual matched load for the characterization of planar discontinuities," in *1992 IEEE MTT-S Int. Microwave Symp. Dig.*, Albuquerque, NM, pp. 1119–1122.
[19] J. R. Mosig, "Integral Equation Technique," in *Numerical Techniques for Microwave and Millimeter-Wave Passive Structures*. New York: John Wiley & Sons, T. Itoh, Ed., 1989, pp. 133–213.
[20] S. Couture, J. C. Beal, and Y. M. M. Antar, "Analysis of dual-frequency stacked patch antennas using subsectional bases," *IEEE Microwave Guided Wave Lett.*, vol. 2, pp. 185–187, May 1992.
[21] F. Alonso-Monferrer, A. A. Kishk, and A. W. Glisson, "Green's functions analysis of planar circuits in a two-layer grounded medium," *IEEE Trans. Antenn. Propagat.*, vol. AP-40, pp. 690–696, June 1992.
[22] D. C. Chang and J. X. Zheng, "Electromagnetic modelling of passive circuit elements in MMIC," *IEEE Trans. Microwave Theory Tech.*, vol. MTT-40, pp. 1741–1747, Sept. 1992.
[23] S. Couture, "The method of moments applied to two-layer microstrip structures," M.Sc.(Eng.) thesis, Queen's Univ. at Kingston, Aug. 1991.
[24] A. W. Glisson and D. R. Wilton, "Simple and efficient numerical methods for problems of electromagnetic radiation and scattering from surfaces," *IEEE Trans. Antenn. Propagat.*, vol. AP-28, pp. 593–603, Sept. 1980.
[25] S. Couture, J. C. Beal, and Y. M. M. Antar, "The cubic spline interpolation of a standing wave envelope," in *1992 IEEE AP-S Int. Symp. Dig.*, Chicago, IL, pp. 196–199.
[26] E. K. L. Yeung, "Multi-layer two-port microstrip discontinuities," M.Sc.(Eng.) thesis, Queen's Univ. at Kingston, Oct. 1992.

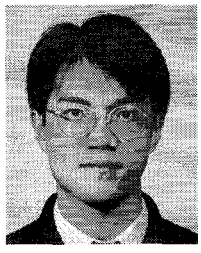

Edwin K. L. Yeung was born in Hong Kong in 1967. He received B.Sc. (Eng.) and M.Sc. (Eng.) degrees in electrical engineering from Queen's Universiry at Kingston, Ontario, Canada, in 1990 and 1992 respectively. He is currently holding a research position at the Royal Military College, Kingston, Ontario, Canada. His research interests in microwaves include the analysis and design of planar microwave circuit components and numerical methods in microwave electromagnetics.

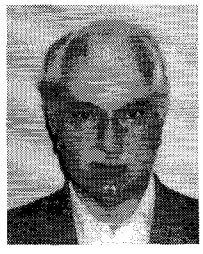

John C. Beal (M'66) was born in London, England in 1933. He received the B.Sc. (Eng.) and Ph.D. degrees in electrical engineering from University College London, London, England, in 1958 and 1964, respectively.

After three years in industry with Redifon, Ltd., in England he joined Colorado State University, Fort Collins, in 1965 as an assistant professor of Electrical Engineering. In 1967 he moved to Queen's University, Kingston, Ontario, Canada, where he is a Professor of Electrical Engineering. Kis research is currently concentrated on the application of numerical methods to the analysis and design of microwave devices.

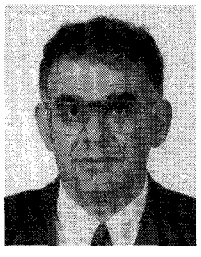

Yahia N. M. Antar (S'73–M'76–SM'85) was born on November 18, 1946 in Meit Temmama, Egypt. He received the B.Sc. (Hons.) degree in 1966 from Alexandria University, Egypt, and the M.Sc. and Ph.D. degrees from the University of Manitoba, Winnipeg, Canada, in 1971 and 1975, respectively, all in electrical engineering.

In 1966, he joined the Faculty of Engineering at Alexandria, where he was involved in teaching and research. At the University of Manitoba he held a University Fellowship, an NRC Postgraduate and postdoctoral Fellowships. In 1976-1977 he was with the Faculty of Engineering at the University of Regina. In June 1977, he was awarded a Visiting Fellowship from the Government of Canada to work at the Communications Research Centre of the Department of Communications, Shirley's Bay, Ottawa, where he was involved in research and development of satellite technology with the Space Electronics group. In May 1979, he joined the Division of Electrical Engineering, National Research Council of Canada, Ottawa, where he worked on polarization radar applications in remote sensing of precipitation, radio wave propagation, electromagnetic scattering and radar cross-section investigations. In November 1987, he joined the staff of the Department of Electrical and Computer Engineering at the Royal Military College of Canada in Kingston, where he is now professor of Electrical Engineering.

He is presently the Chairman of the Canadian CNC, URSI Commission B, and holds adjunct appointments at the University of Manitoba, and at Queen's University in Kingston.